Korean J. Chem. Eng., 32(8), 1528-1541 (2015)
DOI: 10.1007/s11814-015-0028-8

pISSN: 0256-1115
eISSN: 1975-7220

Catalytic cracking of inedible camelina oils to hydrocarbon fuels over bifunctional Zn/ZSM-5 catalysts

Xianhui Zhao, Lin Wei†, James Julson, Zhengrong Gu, and Yuhe Cao

Department of Agricultural and Biosystems Engineering, South Dakota State University, Brookings, South Dakota 57007, USA
(*Received 20 August 2014 • accepted 29 January 2015*)

Abstract−Catalytic cracking of camelina oils to hydrocarbon fuels over ZSM-5 and ZSM-5 impregnated with Zn^{2+} (named bifunctional catalyst) was individually carried out at 500 °C using a tubular fixed-bed reactor. Fresh and used catalysts were characterized by ammonia temperature-programmed desorption (NH_3-TPD), X-ray diffractometer (XRD), Fourier transform infrared spectroscopy (FTIR), scanning electron microscope (SEM) and nitrogen isothermal adsorption/desorption micropore analyzer. The effect of catalysts on the yield rate and qualities of products was discussed. The loading of Zn^{2+} to ZSM-5 provided additional acid sites and increased the ratio of Lewis acid site to Brønsted acid site. BET results revealed that the surface area and pore volume of the catalyst decreased after ZSM-5 was impregnated with zinc, while the pore size increased. When using the bifunctional catalyst, the pH value and heating value of upgraded camelina oils increased, while the oxygen content and moisture content decreased. Additionally, the yield rate of hydrocarbon fuels increased, while the density and oxygen content decreased. Because of a high content of fatty acids, the distillation residues of cracking oils might be recycled to the process to improve the hydrocarbon fuel yield rate.

Keywords: Catalytic Cracking, Camelina, ZSM-5, Zinc, Hydrocarbon

INTRODUCTION

Because of finite reserves of fossil fuels and environmental concern, more and more researchers have explored alternative fuels. Bio-fuel is one such alternative since it has less environmental impact, relatively low cost and available sources, such as vegetable oilseeds, lignocellulosic biomass, and animal fats. The advantages of vegetable oils as alternative fuels include their high heat content, renewability, low sulfur content, low aromatic content, and biodegradability. However, vegetable oils have higher viscosity and lower volatility than usual bio-fuels. Thus, vegetable oils obtained from oilseeds need to be refined to improve these undesirable properties [1,2].

Catalytic cracking is one method that can convert vegetable oils into hydrocarbon fuels. Vegetable oils mainly consist of fatty acids and triglycerides. Through catalytic cracking, triglycerides could be cracked into fatty acids through the decomposition. The long-chain fatty acids would be cracked into short-chain fatty acids, esters, and hydrocarbons. After that, the obtained products would be converted into heavy hydrocarbons, gasoline or light gaseous hydrocarbons [3].

Recently, researchers have reported the conversions of vegetable oils into hydrocarbons over a variety of catalysts. ZSM-5 is a type of molecular-sieve catalyst that has high acidity and a three-dimensional pore system. The internal structure and volume, and small pore size make ZSM-5 difficult to form large aromatic coke precursors inside its pores. ZSM-5 catalyst has been used for triglyceride conversion and widely used in petroleum refinery process [4-7]. There are several reactions occurring inside ZSM-5, including dehydration, decarbonylation and decarboxylation. These reactions can remove oxygen as carbon dioxide, carbon monoxide, and water. Also, the carbon and hydrogen could be converted into aromatics and olefins [8]. The properties of zeolites can be modified with loading metal cations. Zinc-loaded zeolites are suitable catalysts for dehydrogenation of small paraffins and Heck reaction [9]. However, research reports on conversion of vegetable oils to hydrocarbon fuels with Zn modified ZSM-5 catalysts are lacking. $ZnCl_2$ is a moderate strength Lewis acid that has high activity and stereoselectivity. It is nontoxic, cost effective and easily available [10,11]. Lewis acid-Lewis acid catalysts are one type of bifunctional catalysts. Developing active bifunctional catalysts with long lifetime and excellent selectivity is expected to improve the liquid product yield and reduce the cost.

Sharma et al. studied the jatropha oil conversion to liquid hydrocarbon fuels. The sulfide Ni-Mo and Co-Mo catalysts were used for the hydroprocessing of jatropha oil. It was found that catalyst was a significant factor for the performance in terms of yield of kerosene range hydrocarbons [12]. However, using noble metal catalysts and hydrogen will largely increase the processing cost. Li et al. used FCC equilibrium catalyst (zeolite) to produce biofuels from cottonseed oils in a fixed-fluidized bed and concluded that catalytic cracking of cottonseed oils could produce value added products, such as gasoline [13]. Distillation can be used to separate a mixture with wide boiling ranges into products with narrower boiling ranges. The lightest components can be vaporized during heating

†To whom correspondence should be addressed.
E-mail: lin.wei@sdstate.edu

the mixture.

All over the world, a large number of inedible vegetable oils are available. They become quite promising for the sustainable production of bio-fuels since inedible vegetable oils will not cause a debate on food and fuel. In general, inedible vegetable oil sources could be classified into three categories: inedible plant oils (e.g., pongamia glabra oils, babassu oils and lesquerella fendleri oils), waste cooking vegetable oils, and oils of wastes derived from the edible oilseed processing. For example, camelina sativa is one of the inedible oilseed crops so that camelina oil is inedible [14,15]. Also, genetically modified camelina grown on margin lands, such as fallow lands, old mining lands, and irrigation canals, is considered as inedible feedstock. The margin lands require low fertility and water demand for the inedible oil plants to grow. However, fewer researches are found on the conversion of inedible camelina sativa oils (simply called camelina oils in this study, unless specified) into hydrocarbons using a simple catalyst system with low cost.

The objective of this study was to compare the effect of two catalysts, ZSM-5 and its bifunctional zinc-loaded catalyst, on the yield rate and quality of the upgraded camelina oils and hydrocarbon fuels. In this work, camelina oils underwent catalytic cracking using a fixed-bed reactor. Then, a further step of distillation was used to isolate mixed hydrocarbons from the upgraded camelina oils in order to further improve their qualities. The obtained products were characterized. The effect of catalysts on the oil yield rate and properties such as moisture content, density, pH value, dynamic viscosity, oxygen content, heating value and chemical compositions was discussed. Also, the non-condensable gases generated during the catalytic cracking of camelina oils were analyzed.

EXPERIMENTAL

1. Material and Device Preparation

Camelina (sativa) seeds were purchased from Hancock Seed Company, Dade, Florida, USA. The camelina seeds were used for oil extraction immediately after the purchase. The oil extraction was carried out at the Advanced Biofuel Laboratory in the Agricultural and Biosystems Engineering Department, South Dakota State University (SDSU) using a cold press machine (M70 Oil Press, Oil Press Company, Eau Claire, Wisconsin, USA). The camelina oils produced mainly contained linolenic acid, cis-11-eicosenoic acid and stearic acid [16]. After the oil extraction, the produced camelina oils were stored about one month in sealed bottles at room temperature until they were used in the catalytic cracking tests.

2. Catalyst Preparation

Zeolite was purchased from Zeolyst Company, Kansas City, Kansas, USA. The silica-to-alumina atomic ratio in the zeolite was 15 : 1. The ZSM-5 and its bifunctional catalyst doped with 3 wt% Zn^{2+} (ZSM-5-Zn) were prepared using a wet impregnation method [17]. The zeolite was mixed with guar gum and boehmite in a mortar. After they were mixed uniformly, dilute HNO_3 solution and deionized water were added to the mixture dropwise. Then, the mixture was ground and mixed using a pestle until it became a ball. The precursor of Zn^{2+} was zinc chloride powder. For the ZSM-5-Zn ball preparation, the zinc chloride powder was added to the mortar additionally to produce a Zn loading of 3 wt%. The ZSM-5 and ZSM-5-Zn balls were then pressed at 0.69×10^5 Pa (10 psi) through a sieve by a hydraulic press (Owatonna Tool Company), in the shape of strips. The pressed catalysts were sealed and placed at room temperature for 12 h. Then, they were calcined in the air at 550 °C for 4 h. After that, they were stored in a sealed vial in a desiccator, which can minimize the adsorption of the atmospheric moisture. In this study, the fresh calcined ZSM-5 catalyst was used as a control compared to other catalysts [18].

3. Catalyst Characterization

The surface acidity of catalysts was analyzed using a Micrometrics Autochem II Chemisorption Analyzer with a thermal conductivity detector (TCD). The ammonia temperature-programmed desorption (NH_3-TPD) process was pre-programmed into the analyzer. Due to the use of pure NH_3 and carrier gas (e.g. N_2) for the adsorption and desorption analysis, traditional ammonia-TPD methods have some drawbacks, such as complicated testing procedure, uncertainty on low temperature peaks and the influence of physical adsorption on low temperature peaks. To overcome those drawbacks, a modified ammonia-TPD method was used, with ammonia hydroxide instead of pure NH_3 and carrier gas [19-21]. For used catalysts, they were calcined in the air at 600 °C until the coke was removed completely before the analysis in order not to influence the NH_3 desorption. The ammonia adsorption of the catalyst samples was carried out using a wet impregnation method. A sample of 300 mg was added in ammonium hydroxide (28.0-30.0%) and the mixture was placed in a seal state at room temperature for 3 h. The volume ratio of the sample to ammonium hydroxide was 1 : 15. Then, the mixture was dried at 60 °C to remove excess ammonium hydroxide. The dried material was added to the analyzer. Then, helium was purged to remove physically adsorbed impurities such as ammonia, water and CO_2 at 100 °C with a rate of 60 mL/min. After that, the sample was heated linearly at a rate of 10 °C/min from 100 °C to 600 °C under a constant helium flow of 60 mL/min. The sample was held at 600 °C for an additional 34 min. During the period of heating from 100 °C to 600 °C, ample dilute HCl solution (1.0 mol/L) was used to collect the chemisorbed ammonia by the sample. Finally, NaOH solution (0.1 mol/L) was used to titrate the HCl solution to determine the total acid sites of the sample. For each NH_3-TPD profile, the desorption peak fitting and data analysis were carried out using Lorentzian fitting with Origin8 software (OriginLab Corporation). The carbon (C) content of used ZSM-5 and used ZSM-5-Zn catalysts were determined using a CE-440 Elemental Analyzer (Exeter Analytical, Inc.), according to ASTM D4057. The combustion temperature and reduction temperature were 1,040 °C and 700 °C, respectively. The purge time and combustion time were 60 s and 90 s, respectively. The fill time was in the range of 20-50 s. The oxygen pressure and helium pressure was 1.72×10^5 Pa (25 psi) and 1.17×10^5 Pa (17 psi), respectively. The test of each sample was conducted in duplicate.

Automated multipurpose X-ray diffractometer (XRD, SmartLab, Rigaku Corporation) was used to examine the catalysts. The scan range was 5-50 degrees at a scan speed of 2°/min. The Fourier transform infrared spectroscopy (FTIR) spectra of catalysts were performed on a Nicolet 6700 FT-IR spectrometer using KBr pellets. The surface area, pore volume, and pore size of catalysts were measured with a Micromeritics TriStar 3000 automated gas adsorp-

tion analyzer. For used catalysts, they were not directly measured since the catalyst coking would pollute the column in the analyzer. Therefore, used catalysts were calcined in the air at 600 °C until the coking was removed completely before the analysis. Physisorption analysis with nitrogen (liquid nitrogen bath) was carried out using an ASAP 2010 Micropore analyzer at 77 K. Catalyst samples were first degassed using a Micromeritics FlowPrep 060 unit at 200 °C for a minimum of 5 h to make sure that any moisture was removed prior to nitrogen isotherm analyses. The surface area was calculated using a Brunauer-Emmett-Teller (BET) model for the nitrogen adsorption isotherm. The pore size distribution was determined using a Barrett-Joyner-Halenda (BJH) adsorption model. The single point adsorption total pore volume of pores smaller than 933.3 Å diameter was obtained at a relative pressure of P/P_0=0.979. The adsorption average pore diameter was calculated by $4V_T/S_{BET}$ [18,22]. The surface morphology of catalysts was characterized using a scanning electron microscope (SEM, Hitachi S-3400N).

4. Experiment Procedure

The catalytic cracking of camelina oils was carried out in a fixed-bed reactor. A simplified schematic diagram of this fixed-bed reactor system is shown in Fig. 1. The fixed-bed reactor system was composed of four parts: oil sample injection, preheating, catalytic reaction and products collection. In this study, two different catalysts, ZSM-5 and ZSM-5-Zn, were used at a typical reaction temperature of 500 °C. The camelina oils were pumped into a preheater with the carrier gas of N_2. The liquid hourly space velocity (LHSV) was set as 1.0 h^{-1}. The temperature of the preheater was 450 °C. A continuous flow of nitrogen was maintained at 1.38×10^5 Pa (20 psi). Before camelina oils were pumped, nitrogen was blown for 15 min to remove the air throughout the reactor system. Also, the preheater and reactor would have reached the corresponding temperatures for 30 min so that the later catalytic reactions could take place better. Camelina oils became oil vapors after flowing through the preheater and then the oil vapors went through the reactor. The preheater could be helpful for the oil vapors to contact well with the catalyst in the reactor. The reactor was a stainless steel tube, fixed coaxially in a furnace. The length and the internal diameter of the tube were 508 mm and 25.4 mm, respectively. The oil vapors were catalytically cracked in the reactor with the activation of the catalyst, whose amount was 60 mL. The produced oil gases, such as small hydrocarbon molecules, were cooled. Condensed oil gases were collected in the form of liquids through a condenser system. The refrigerated circulator's temperature in this condenser system was set as −10.0 °C. Some oil gases could not be condensed in this condenser system and they were considered as non-condensable gases. The non-condensable gases, including H_2, C_1-C_5, CO and CO_2, flowed through a filter in order to avoid the environmental pollution. Part non-condensable gases would be collected using a gas sampling bag for their composition analysis [18].

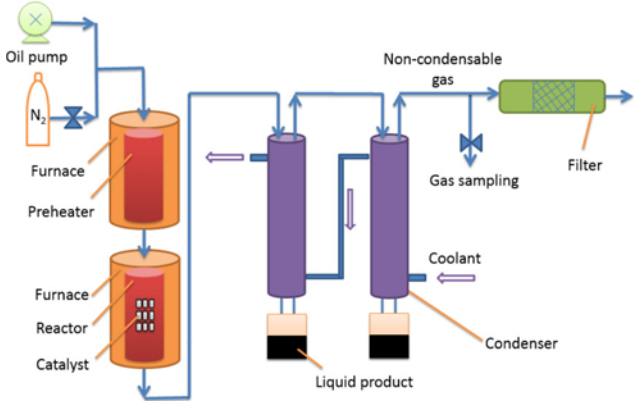

Fig. 1. Schematic diagram of the fixed-bed reactor system.

After the catalytic cracking of camelina oils, there were two phases in the collected liquid product. The top oil phase was considered as upgraded camelina oils and the lower phase was mainly water. The obtained upgraded camelina oils were then distilled at 230 °C in order to obtain hydrocarbons with carbon numbers lower than 13 for future bio-fuel production. During the distillation, small molecules with low boiling points became vapors. These vapors flowed into an overhead condenser and were cooled back into a liquid. The liquid was collected and considered as hydrocarbon fuels. The large molecules with high boiling points were too heavy to vaporize under this distillation condition. They were left in the distillation flask and considered as distillation residues [18].

5. Data Collection

The upgraded camelina oils produced over ZSM-5 (UCO), upgraded camelina oils produced over ZSM-5-Zn (UCOZ), hydrocarbon fuels produced over ZSM-5 (HF), hydrocarbon fuels produced over ZSM-5-Zn (HFZ), distillation residues produced over ZSM-5 (DR) and distillation residues produced over ZSM-5-Zn (DRZ) were characterized by testing their pH value, dynamic viscosity, moisture content, density, main chemical compositions, oxygen content and heating value.

The pH values of samples were determined using a pHTestr 20 (Fisher Scientific) and pH testing papers. The dynamic viscosity was measured with a Viscoanalyzer (REOLOGICA Instruments AB Company) at 20 °C. The moisture content was tested using a Karl Fischer Titrator V20 (Mettler Toledo Company) at room temperature, according to ASTM E1064. The density was tested three times by the ratio of sample mass to sample volume at room temperature. The average value of these three tests was used as the density [16].

The major chemical compositions of samples were analyzed by gas chromatography-mass spectrometry (GC-MS) (Agilent GC-7890A and MSD-5975C). The capillary columns were 30 m×0.25 mm×0.25 μm DB-5MS and the carrier gas was hydrogen with a flow rate of 1 mL/min. Before being tested, the samples were pretreated with derivatization to make the polar compounds volatile enough. Samples with 0.03 g were added in a container and 4 mL hexane (with purity of 95%) were added as a solvent. The obtained mixture was shaken for 2 min. Then 2 mL CH_3OH (99.9%, extra pure) and 2 mL boron trifluoride (12%, 1.5 M) in methanol were added in the mixture. After that, the mixture was heated in a water bath at 60 °C for 5 min. After the mixture cooled, 1 mL distilled water and 2 mL hexane were added to remove the excess of reagents. Then the mixture was centrifuged at 2,500 g for 10 min to obtain the organic phase. The organic phase was taken out and dried using anhydrous sodium sulfate. Finally, about 1.5 mL organic phase without water was filtered into a vial for the GC-MS test. The GC-MS test parameters were as follows. One microliter organic phase was

introduced through an injection port operated in a splitless mode. The inlet temperature was 285 °C and the splitless time was 30 s. The original column temperature was 175 °C and it was held for 6 min. Then, it became 260 °C after 5.667 min at a speed rate of 15 °C/min. The hold time at 260 °C was 15.68 min. The total run time was 27.347 min. The major chemical compositions of samples were identified through the NIST Mass Spectral library and literatures [23,24].

The oxygen (O) content of samples was determined using a CE-440 Elemental analyzer, according to ASTM D4057. Acetanilide was used as a calibration standard sample. The combustion temperature and reduction temperature were 950 °C and 670 °C, respectively. The purge time and combustion time were 50 s and 40 s, respectively. Helium was used to purge the instrument and carry the combustion product from the analytical system to atmosphere. The helium pressure was 1.17×10^5 Pa (17 psi). The fill time was 40-50 s. The sample was sealed in a silver capsule within a nickel sleeve [16].

The heating value of samples was measured with a calorimeter system (C 2000, IKA-Works, Inc.), based on ASTM D4809. About 0.5 g sample was added in a crucible and placed in a decomposition vessel. The sample was ignited with a cotton twist. The heating value was calculated based on the temperature change of water inside the measuring cell.

The chemical compositions of generated non-condensable gases were measured with a gas chromatography (GC) System. An Agilent GC (7890A) with a flame ionization detector (FID) and a thermal conductivity detector (TCD) were used. Nitrogen was used as the carried gas for FID and helium was used as the carried gas for TCD. The FID is used for the analysis of C_1-C_5 hydrocarbons. The TCD is used for measuring H_2, CO, CO_2, O_2, N_2 and H_2S [25].

The yield rates of products generated during the catalytic cracking process were defined by the following equations:

Yield rate of upgraded camelina oils=(mass of oil phase after upgrading/ mass of camelina oil feed)×100% (1)

Yield rate of hydrocarbon fuels=(mass of hydrocarbon fuels/ mass of upgraded camelina oil feed)×100% (2)

Yield rate of distillation residues=(mass of distillation residues/ mass of upgraded camelina oil feed)×100% (3)

RESULTS AND DISCUSSION

1. Characterization of Catalysts

1-1. Surface Acidity and Carbon Content Analysis

The NH_3-TPD profiles of catalysts are shown in Fig. 2. All of these four catalysts exhibited three acid sites with different acid strength. Generally, the peak temperature was related to the strength of acid sites. There was no big difference among the TPD profiles of fresh calcined ZSM-5, used ZSM-5 and used ZSM-5-Zn. For these three catalysts, their peaks centered at around 181 °C, 332 °C and 595 °C were assigned to NH_3 desorption from weak acid sites, medium acid sites and strong acid sites, respectively. The TPD profile of used ZSM-5-Zn indicated that some Zn^{2+} might be lost during the process of coke removal. The coke on used ZSM-5-Zn led to several chemical reactions through gasification to produce carbon monoxide and carbon dioxide [26]. The exothermicity of these reactions, which generally cause overheating and high temperature higher than 950 °C, might result in the formation of zinc vapors and cause the loss of Zn^{2+}. For fresh calcined ZSM-5-Zn, its peak assigned to NH_3 desorption from strong acid sites appeared at a similar temperature to other three catalysts. However, the peaks assigned to NH_3 desorption from weak acid sites and medium acid sites shifted towards higher temperatures (around 219 °C and 384 °C, respectively). The corporation of Zn^{2+} to ZSM-5 might induce extra-framework aluminum species, which might increase the strength of acid sites and then retain the ammonia more strongly. The presence of Lewis acid sites on ZSM-5 could be assigned to zeolite framework sites or to extra-framework aluminum species [27].

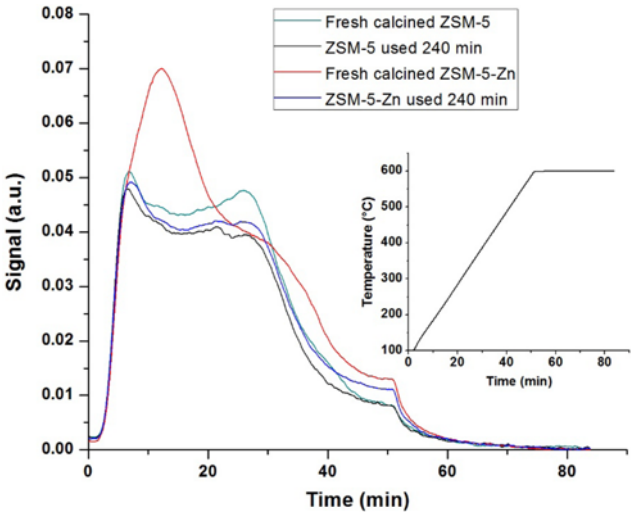

Fig. 2. NH_3-TPD profiles of catalysts with heating rate of 10 °C/min from 100 °C to 600 °C and holding at 600 °C for 34 min.

The total acid sites and the ratio of Lewis acid site to Brønsted acid site (L/B ratio) are presented in Table 1. The peak temperature and L/B ratio were determined by deconvolution and subse-

Table 1. Surface acidity of the catalysts

Catalyst	Low peak temperature (°C)	Medium peak temperature (°C)	High peak temperature (°C)	Total acid sites (mmol/g)	Lewis: Brønsted ratio
Fresh calcined ZSM-5	181	334	600	0.52	0.17
ZSM-5 used 240 min	180	328	596	0.36	0.18
Fresh calcined ZSM-5-Zn	219	384	597	0.63	0.65
ZSM-5-Zn used 240 min	182	334	589	0.50	0.17

quent integration of desorption peaks. Based on other researchers' findings, the weak acid sites, medium acid sites and strong acid sites of the four catalysts in this study could be attributed to Lewis acid sites, Brønsted acid sites and Brønsted acid sites, respectively [28-31]. Fresh calcined ZSM-5-Zn catalyst had higher total acid sites than fresh calcined ZSM-5 catalyst. It meant that the loading of Zn^{2+} to ZSM-5 provided additional acid sites. High acid sites are vital for the catalytic cracking of inedible vegetable oils to biofuels. Used catalysts had lower acid sites compared to fresh catalysts, which indicated that the surface acidity of catalysts would decrease after the catalytic cracking use. However, the used catalysts still possessed a certain surface acidity so that they might be recycled for further catalytic cracking of camelina oils, especially after the future optimization of the regeneration process to avoid extreme high temperatures during the gasification of the coke. There was no big difference among the L/B ratios of fresh calcined ZSM-5, used ZSM-5 and used ZSM-5-Zn. However, fresh calcined ZSM-5-Zn catalyst exhibited a much higher L/B ratio than that of other three catalysts, which might be because some Brønsted acid protons of ZSM-5 were substituted by Zn^{2+}. Another reason could be the formation of extra-framework aluminum species that resulted in a higher concentration of Lewis acid sites.

Carbon accumulation, which was considered as coke in this study, on the catalysts involved a complex process such as hydrocarbon polymerization and dehydrogenation. The coke accumulated on the surface and the porous structure of the ZSM-5 and ZSM-5-Zn catalysts. It would influence the activity of catalysts by covering some of their active sites and/or blocking some of their channels. The carbon content of used ZSM-5 and used ZSM-5-Zn was 13.9% and 14.9%, respectively. The higher conversion of camelina oils to hydrocarbon fuels over ZSM-5-Zn indicated the higher activity of ZSM-5-Zn, which might lead to the higher coke yield. This result was consistent with the finding of Al-Khattaf [32]. During the catalytic cracking of camelina oils, light hydrocarbons such as C_3H_6 and C_4H_8 were produced. The ZSM-5 and ZSM-5-Zn catalysts might adsorb these light hydrocarbons. Then, these hydrocarbons polymerized together to form coke. During these condensation reactions, dehydrogenation or hydrogen transferring might take place.

1-2. XRD Analysis

Fig. 3 represents the XRD spectra of four catalysts, including fresh calcined ZSM-5, used ZSM-5, fresh calcined ZSM-5-Zn and used ZSM-5-Zn. For fresh calcined ZSM-5 catalyst, the main peaks were observed at 2θ=8.04°, 2θ=8.89°, and 2θ=23.2°. The peak position and intensity of the catalyst were in good accord with the previously reported spectrum of the zeolite [11,33,34]. There was no obvious difference between the bulk structures of fresh calcined ZSM-5 and fresh calcined ZSM-5-Zn. No peaks related to the Zn^{2+} were found from the X-ray diffractograms. It indicated that the incorporation of 3 wt% Zn^{2+} did not apparently change the structure of the parent catalyst, ZSM-5. The XRD pattern of the ZSM-5-Zn indicated that the structure of the ZSM-5 remained intact after being doped with 3 wt% Zn^{2+}. These XRD patterns revealed that Zn^{2+} was dispersed on the ZSM-5 catalyst. The finding is in accord with the suggestions made by Jiang et al. [35]. However, the peak intensities of fresh calcined ZSM-5 and fresh calcined ZSM-5-Zn were slightly different, which might be due to a certain absorption coefficient of Zn^{2+}.

Even though the fresh calcined ZSM-5 and fresh calcined ZSM-5-Zn were used in the fixed-bed reactor for 240 min, their bulk structures did not change largely, shown in Fig. 3. The ZSM-5 and ZSM-5-Zn retained their major structural elements after the catalytic cracking reactions. This finding indicated that the used catalysts might be recycled for the future catalytic cracking use in the fixed-bed reactor.

1-3. FT-IR Spectra

The infrared study range between 4,000 cm^{-1} and 400 cm^{-1}, focused on the framework vibrations of catalysts, was performed. As shown in Fig. 4, there was no big band position shifts between these four types of catalysts. It meant no isomorphous substitution in the ZSM-5 framework took place. It supports the prior discussion on XRD of catalysts that the framework of ZSM-5 remained intact.

For all of the catalysts, the water-bending vibration at 1,632 cm^{-1} was observed. This indicated that the adsorbed water was presented

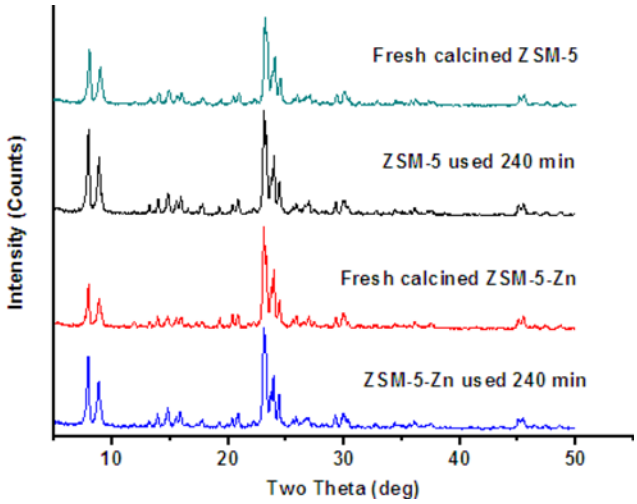

Fig. 3. XRD spectra of the catalysts.

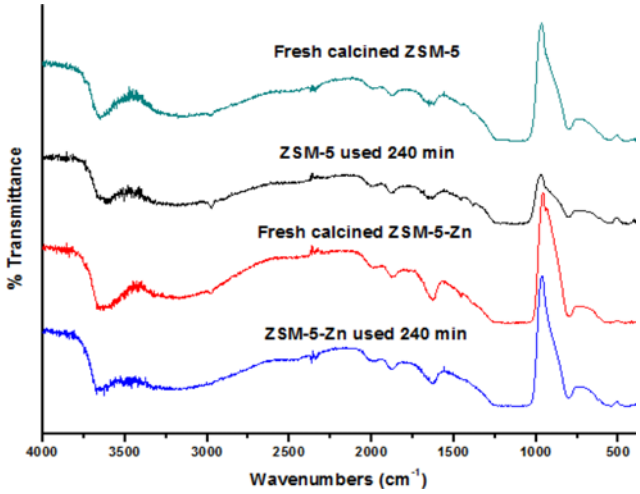

Fig. 4. FTIR spectra of the catalysts.

in the catalyst samples, which might occur during the incipient wet impregnation process. Also, the Si-O-Si symmetric stretching vibration at 796 cm^{-1} was observed. This band might be related to the internal linkages in SiO_4 or AlO_4 of the ZSM-5 lattices [18,36]. The band near 546 cm^{-1} (double ring vibration) was presented for all catalysts, which indicated the formation of only ZSM-5 phase. It might be because the presence of zinc was not sufficient to be detected.

All of the catalysts exhibited an O-H group in the band at 3,600-3,620 cm^{-1}. This mainly resulted from the framework of bridged hydroxyl groups. The O-H group might originate from the framework of Al or the adsorbed water [11]. The O-H group indicated the existence of the catalytic activity. They also indicated that the catalysts possessed a large number of acid sites, which were significant for the catalytic cracking reactions to take place. The band at ~3,635 cm^{-1} was associated with the Si-OH group. It indicated that zinc was only incorporated on the external surface of the ZSM-5 framework.

1-4. BET and BJH Analysis

Table 2 shows the surface area, pore volume and pore size of catalysts. The surface area and pore volume of fresh calcined ZSM-5-Zn were smaller than those of fresh calcined ZSM-5. The pore size of fresh calcined ZSM-5-Zn was slightly larger than that of fresh calcined ZSM-5. This indicated that maybe the introduction of Zn^{2+} blocked some micro-pores of ZSM-5 so that the meso-pores would occupy more. Under this situation, the pore size of fresh calcined ZSM-5-Zn became slightly higher, while the pore volume and surface area became smaller, compared to fresh calcined ZSM-5. After being used for 240 min, the surface area, pore volume and pore size of used catalysts increased compared with fresh calcined catalysts. This might be because the flow of oil vapors expanded the pore structures of the catalysts during the catalytic cracking process so that some mesopores of the catalysts became larger. The above results also indicated that the used catalysts might be recycled for further use in the future.

Table 2. The BET and BJH analysis of the catalysts

Catalyst	S_{BET} [a] (m^2/g)	V_T [b] (cm^3/g)	$d_{average}$ [c] (Å)
Fresh calcined ZSM-5	417.0	0.398	38.1
ZSM-5 used 240 min	418.8	0.436	41.6
Fresh calcined ZSM-5-Zn	375.4	0.362	38.6
ZSM-5-Zn used 240 min	421.4	0.413	39.2

[a]BET surface area

[b]The single point adsorption total pore volume of pores less than 908 Å diameter, measured at P/P_0=0.979

[c]Adsorption average pore diameter, calculated by 4 V_T/S_{BET}

The N_2 adsorption and desorption isothermal curves of cata-

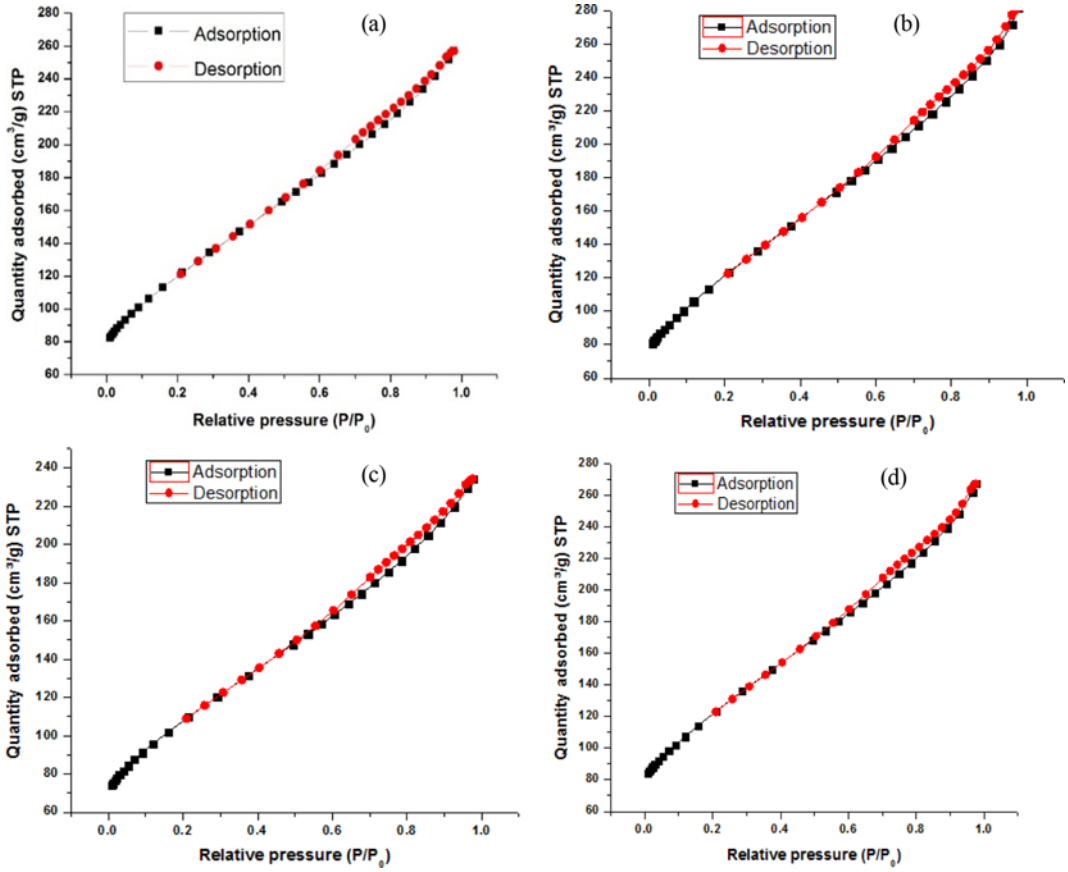

Fig. 5. Adsorption and desorption isotherm of nitrogen at 77 K, on the catalysts: (a) Fresh calcined ZSM-5; (b) ZSM-5 used 240 min; (c) fresh calcined ZSM-5-Zn; and (d) ZSM-5-Zn used 240 min.

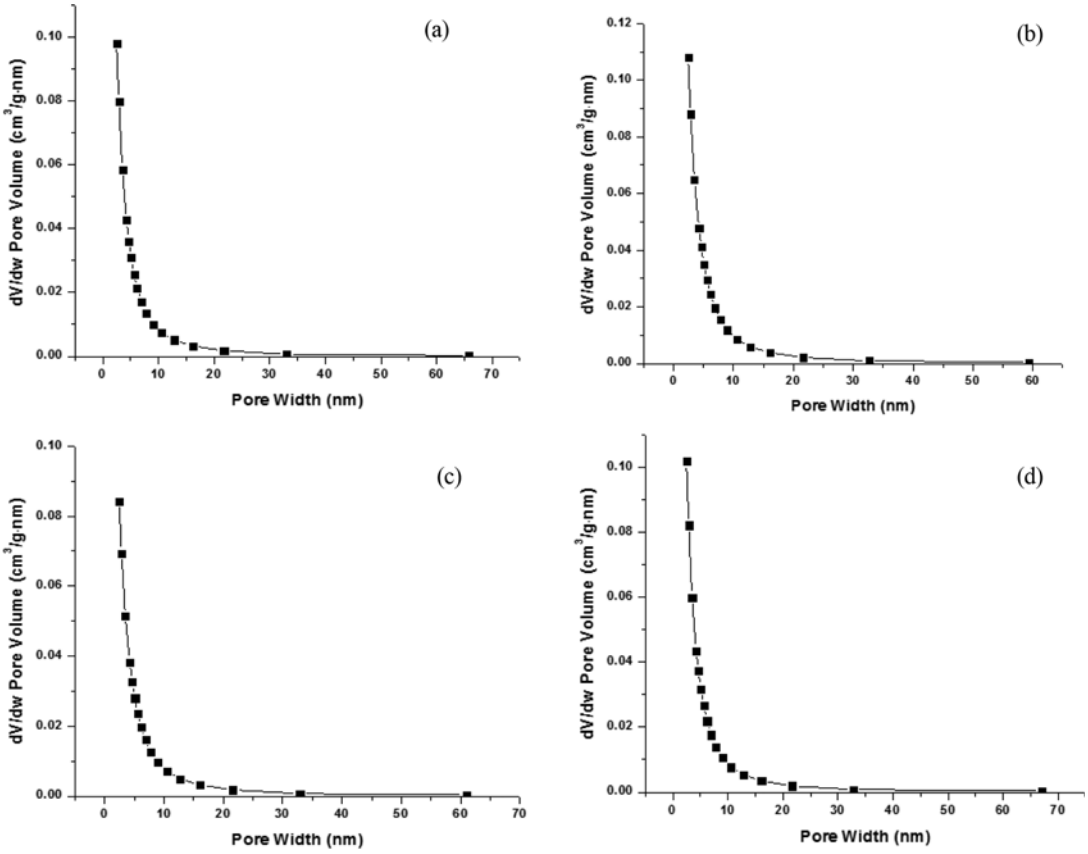

Fig. 6. BJH pore size distribution of the catalysts: (a) fresh calcined ZSM-5; (b) ZSM-5 used 240 min; (c) fresh calcined ZSM-5-Zn; and (d) ZSM-5-Zn used 240 min.

lysts are shown in Fig. 5. According to the IUPAC classification of physisorption isotherms, all of the catalysts exhibited a combination of type I and type IV isotherm with enhanced uptake of nitrogen at a higher relative pressure. The adsorption quantity at low relative pressures (p/p_0) was high, which indicated the presence of microporous adsorption. The curves were accompanied by a hysteresis loop between the relative pressures of 0.5-1.0. This might be due to the crystalline agglomerates, which resulted in the mesoporous structure. A remarkable increase of the adsorption quantity in the low relative pressure region and the hysteresis loop in the high relative pressure region indicated the presence of both micropores and mesopores [18]. There was no big difference between the isothermal curves of all catalysts. The BJH pore size distribution of the catalysts is presented in Fig. 6. The BJH pore size model also confirmed the presence of mesoporosity in all of the catalysts. Also, there was no big difference between the pore size distributions of all catalysts. Thus, the isothermal type for all of the catalysts was considered as a combination of type I and type IV.

1-5. SEM Analysis

To obtain the catalysts' morphologies and to assess the reliability of XRD data, an SEM experiment for comparing the structural properties of the catalysts was performed. Fig. 7 displays the surface morphologies of catalysts. The difference in each pair of the SEM images is the magnitude scale. The catalysts consisted of the agglomeration of ZSM-5 particles. The catalysts were spherical structure and contained small pores. Also, they had a cube-like morphology and the small particles were interconnected with each other.

There was no big difference between the surface morphologies of fresh calcined ZSM-5 and fresh calcined ZSM-5-Zn. It revealed that there were no zinc oxides inside the catalyst as a discrete phase. It also proved the high dispersion of cations in the ZSM-5 catalyst, as evoked by XRD data. The fresh calcined ZSM-5 contained some cracks. There were cauliflower-like particles on the top surface of fresh calcined ZSM-5. For fresh calcined ZSM-5-Zn, there were also similar particles on the top surface. This finding corresponds with the XRD patterns.

After the catalytic cracking, the surface morphologies of used ZSM-5 and used ZSM-5-Zn were similar. However, the used ZSM-5 had more particles on the top surface than those of used ZSM-5-Zn. Both the used ZSM-5 and used ZSM-5-Zn became more compact than the fresh calcined ZSM-5 and fresh calcined ZSM-5-Zn, respectively. Also, the micro-surface of the used ZSM-5 and used ZSM-5-Zn looked smoother with fewer particles on their top surface. Perhaps, the flow of oil vapors during the catalytic cracking process washed the catalyst surface and made it cleaner.

2. Main Chemical Compositions of Products

Table 3 shows the major chemical compositions in the upgraded camelina oils, hydrocarbon fuels and distillation residues produced over ZSM-5 and ZSM-5-Zn, respectively. The upgraded camelina oils, produced over ZSM-5 and ZSM-5-Zn using the catalytic crack-

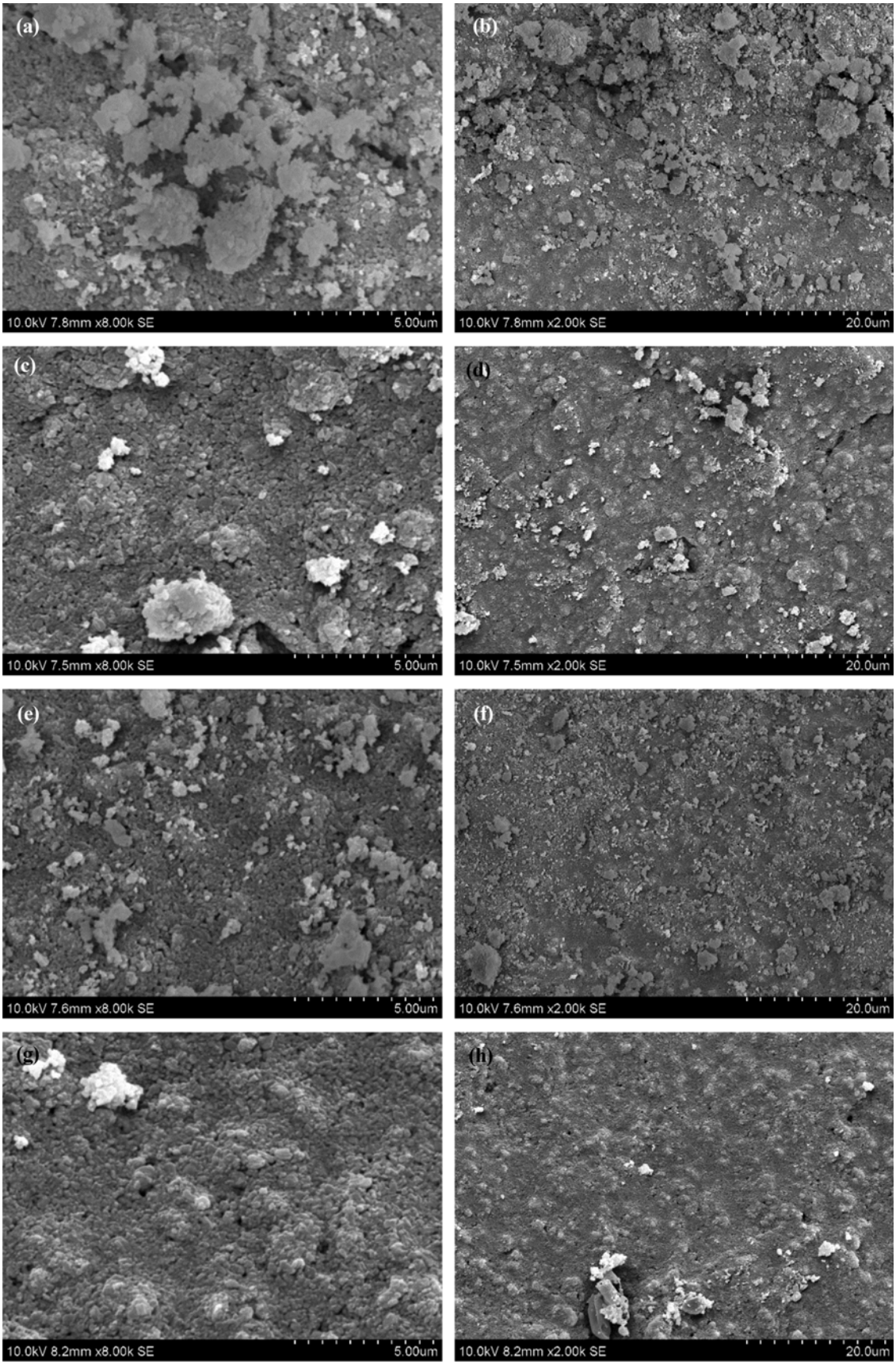

Fig. 7. SEM images of catalysts with different magnitude scales: fresh calcined ZSM-5 (a), (b); ZSM-5 used 240 min (c), (d); fresh calcined ZSM-5-Zn (e), (f); and ZSM-5-Zn used 240 min (g), (h).

Table 3. Main chemical compositions of products produced over two catalysts

	ZSM-5		ZSM-5-Zn	
	Component	Area %	Component	Area %
Upgraded oils	Tetracyclo[4.2.1.0(3,7).0(2,9)]non-4-ene, 4-phenyl- ($C_{15}H_{14}$)	0.57	Hexadecanoic acid ($C_{16}H_{32}O_2$)	12.4
	Hexadecanoic acid ($C_{16}H_{32}O_2$)	6.16	Oleic acid ($C_{18}H_{34}O_2$)	60.0
	Oleic acid ($C_{18}H_{34}O_2$)	66.8	Gibberellic acid ($C_{19}H_{22}O_6$)	8.75
	Octadecanoic acid ($C_{18}H_{36}O_2$)	19.4	Androstenediol ($C_{19}H_{30}O_2$)	4.43
	Methyl 18-methylnonadecanoate ($C_{21}H_{42}O_2$)	0.66	Methyl 11-eicosenoate ($C_{21}H_{42}O_2$)	4.18
	9-Octadecenamide, (Z)- ($C_{18}H_{35}NO$)	1.21	Methyl 18-methylnonadecanoate ($C_{21}H_{42}O_2$)	3.01
	Methyl 20-methyl-heneicosanoate ($C_{23}H_{46}O_2$)	1.84	9-Octadecenamide, (Z)- ($C_{18}H_{35}NO$)	1.90
	11-Hexacosyne ($C_{26}H_{50}$)	2.79	2,6,10,14,18,22-Tetracosahexaene, 2,6,10,15,19,23-hexamethyl-, (all-E)-, didehydro deriv. ($C_{30}H_{48}$)	5.38
	4,5,11,12-Tetrahydrobenzo[a]pyrene ($C_{20}H_{16}$)	0.57		
Hydrocarbon fuels	Bi-2,4,6-cycloheptatrien-1-yl ($C_{14}H_{14}$)	0.81	2H-Pyran-2-one, 5-ethylidenetetrahydro-4-(2-hydroxyethyl)- ($C_9H_{14}O_3$)	0.48
	Hexadecanoic acid ($C_{16}H_{32}O_2$)	5.88	Hexadecanoic acid ($C_{16}H_{32}O_2$)	12.1
	2H-Inden-2-one, octahydro-3a-methyl-, cis- ($C_{10}H_{16}O$)	1.13	11-Octadecenoic acid ($C_{18}H_{34}O_2$)	1.27
	9-Octadecenoic acid (Z)- ($C_{18}H_{34}O_2$)	4.07	Octadecanoic acid ($C_{18}H_{36}O_2$)	5.48
	Heptadecanoic acid, 16-methyl ($C_{18}H_{36}O_2$)	6.77	4,7-Methano-1H-indene, octahydro- ($C_{10}H_{16}$)	0.11
	Cyclohexane, (2,2-dimethylcyclopentyl)- ($C_{13}H_{24}$)	1.76	Aromadendrene ($C_{15}H_{24}$)	0.17
	9-Octadecenamide, (Z)- ($C_{18}H_{35}NO$)	3.96	1-Nonadecene ($C_{19}H_{38}$)	3.02
	Hexane, 2,3-dimethyl- (C_8H_{18})	73.5	Eicosanoic acid ($C_{20}H_{40}O_2$)	0.55
	3-Octyne, 5-methyl- (C_9H_{16})	0.10	9-Octadecenamide, (Z)- ($C_{18}H_{35}NO$)	8.39
	1-Octadecyne ($C_{18}H_{34}$)	0.13	Hexane, 2,3-dimethyl- (C_8H_{18})	68.4
	3,4-Octadiene, 7-methyl- (C_9H_{16})	0.10	1,3,5-Hexatriene, 3-methyl-, (Z)- (C_7H_{10})	0.08
	cis-3-Methyl-exo-tricyclo[5.2.1.0(2.6)]decane ($C_{11}H_{18}$)	0.07		
	Tricyclo[5.3.0.0(3,9)]dec-4-ene ($C_{10}H_{14}$)	0.09		
	1-Cyclohexylnonene ($C_{15}H_{28}$)	0.09		
	3-Cyclopentyl-1-propyne (C_8H_{12})	0.07		
	1,2,5-Oxadiazol-3-amine, 4-(3-methoxyphenoxy)- ($C_{19}H_{36}$)	0.08		
	1,5,9,13-Tetradecatetraene ($C_{14}H_{22}$)	0.07		
	Limonene ($C_{10}H_{16}$)	0.08		
	1,5-Hexadiene, 2,5-dipropyl- ($C_{12}H_{22}$)	0.07		
	Tricyclo[4.2.2.1(2,5)]undecane ($C_{11}H_{18}$)	0.10		
	Bicyclo[5.1.0]oct-3-ene (C_8H_{12})	0.17		
	2-Octyne (C_8H_{14})	0.18		
	3-Tridecen-1-yne, (Z)- ($C_{13}H_{22}$)	0.09		
	1,5-Hexadiyne (C_6H_6)	0.08		
	3-[(Z)-1-Butenyl]-4-vinylcyclopentene ($C_{11}H_{16}$)	0.08		
	Methyl ethyl cyclopentene (C_8H_{14})	0.09		
	Bicyclo[3.2.0]hept-6-ene (C_7H_{10})	0.08		
	cis-1,4-Dimethyl-2-methylenecyclohexane (C_9H_{16})	0.09		
	3-Hexyne (C_6H_{10})	0.11		
	1,4-Heptadiene (C_7H_{12})	0.11		

ing method, were a mixture mainly containing hydrocarbons and oxygenates. In camelina oils, linolenic acid, cis-11-eicosenoic acid and stearic acid were the main components. After the catalytic cracking, these fatty acids were mainly converted into short-chain fatty

Table 3. Continued

	ZSM-5		ZSM-5-Zn	
	Component	Area %	Component	Area %
Distillation residues	Tricyclo[4.2.1.0(2,5)]nona-3,7-diene, 9-methoxy-1-phenyl- ($C_{16}H_{16}O$)	10.6	N-2,4 Dnp-L-arginine ($C_{12}H_{16}N_6O_6$)	6.53
	5,7,9(11)-Androstatriene, 3-hydroxy-17-oxo ($C_{19}H_{24}O_2$)	8.42	Oleic acid ($C_{18}H_{34}O_2$)	58.9
	Pectenin ($C_{13}H_{19}NO_2$)	11.7	Octadecanoic acid ($C_{18}H_{36}O_2$)	4.51
	Oleic acid ($C_{18}H_{34}O_2$)	63.4	Linoleic acid ethyl ester ($C_{20}H_{36}O_2$)	2.08
	Tetraneurin D ($C_{17}H_{24}O_6$)	3.67	cis-11-Eicosenoic acid ($C_{20}H_{38}O_2$)	23.6
	2,6,10,14,18,22-Tetracosahexaene, 2,6,10,15,19,23-hexamethyl-, (all-E)-, didehydro deriv. ($C_{30}H_{48}$)	2.15	i-Propyl 5,9,17-hexacosatrienoate ($C_{29}H_{52}O_2$)	1.21

acids, esters, and hydrocarbons. For upgraded camelina oils produced over ZSM-5, the total fatty acids occupied 92.36%. The hydrocarbons, C_{15}, C_{20} and C_{26}, occupied 3.93% in total. For upgraded camelina oils produced over ZSM-5-Zn, the total fatty acids occupied 81.15%. The hydrocarbon of C_{30} occupied 5.38%. The total hydrocarbon content in upgraded camelina oils produced over ZSM-5-Zn was higher than that in upgraded camelina oils produced over ZSM-5. However, upgraded camelina oils produced over ZSM-5 and upgraded camelina oils produced over ZSM-5-Zn contained the same main composition, which was oleic acid. It indicated that linolenic acid contained in camelina oils was hydrogenated to oleic acid during the catalytic cracking process.

After the distillation treatment, there was a much higher content of hydrocarbons in hydrocarbon fuels compared to upgraded camelina oils. For hydrocarbon fuels produced over ZSM-5, there were a number of types of hydrocarbons produced that were distributed from C_6 to C_{19}. Their total area content of hydrocarbons reached 78.2%. For hydrocarbon fuels produced over ZSM-5-Zn, the total content of hydrocarbons was 71.78%. For both hydrocarbon fuels produced over ZSM-5 and hydrocarbon fuels produced over ZSM-5-Zn, the total content of fatty acids and other oxygenates decreased largely compared to upgraded camelina oils. It proved that the distillation treatment could separate small molecules with low boiling points from the upgraded camelina oils. For hydrocarbon fuels produced over ZSM-5 and hydrocarbon fuels produced over ZSM-5-Zn, their main chemical component was the same while there was a difference between other components. It indicated that doping 3 wt% Zn to ZSM-5 had a certain effect on the chemical compositions of hydrocarbon fuels, which might be because the acid sites of the catalyst were changed after the Zn^{2+} doping. For distillation residues, they mainly contained large molecules such as fatty acids and esters which were left in the distillation flask. Both distillation residues produced over ZSM-5 and distillation residues produced over ZSM-5-Zn mainly contained oleic acid, which was the same to that in upgraded camelina oils. The distillation residues might be recycled for a second catalytic cracking since they contained a high content of fatty acids.

3. Oxygen Content of Products

Table 4 represents the oxygen content of products produced over ZSM-5 and ZSM-5-Zn, respectively. The oxygen content of camelina oils was used as a reference for comparison [16]. Camelina oils contain a high oxygen content, 12.4%. The oxygen content affects the specific energy and the combustion of oils [37]. During the catalytic cracking, some oxygen atoms in camelina oils were removed in the form of H_2O, CO and CO_2. Some produced H_2O was dissolved in the upgraded camelina oils. Other produced H_2O precipitated in the water phase of the collected liquid product. CO and CO_2 evaporated away as the compositions in the non-condensable gases. Compared to camelina oils, the oxygen content of upgraded camelina oils decreased. It indicated that ZSM-5 and ZSM-5-Zn were effective to reduce the oxygen content in camelina oils. After the catalytic cracking, the oxygen content of hydrocarbon fuels decreased further. The oxygen content of hydrocarbon fuels produced over ZSM-5-Zn was lower than that of hydrocarbon fuels produced over ZSM-5. It indicated that doping 3 wt% Zn^{2+} to ZSM-5 was helpful to reduce the oxygen content of hydrocarbon fuels. The oxygen content of distillation residues was higher than that of upgraded camelina oils since the large molecules were left in the distillation flask.

Table 4. Oxygen content of products produced over two catalysts

Catalyst	O (wt%) *Camelina oils: 12.4±0.78		
	Upgraded oils	Hydrocarbon fuels	Distillation residues
ZSM-5	9.39±0.58	4.49±2.65	9.46±1.05
ZSM-5-Zn	9.29±1.24	4.07±0.21	10.8±1.13

4. Physical Properties of Products

As shown in Table 5, the pH values of upgraded camelina oils produced over two different catalysts were measured. The properties of camelina oils in Table 5 were used as a reference for comparison [16]. It is obvious that the upgraded camelina oils produced over both ZSM-5 and ZSM-5-Zn showed a mild acidity. However, the pH value of upgraded camelina oils produced over ZSM-5-Zn was slightly higher than that of upgraded camelina oils produced over ZSM-5. Upgraded camelina oils produced over ZSM-5-Zn contained a lower area content of fatty acids, which might cause the higher pH value. The upgraded camelina oils showed lower pH values compared to camelina oils. Perhaps the split of triglycerides that were derived from camelina oils resulted in the higher acidity of upgraded camelina oils. After the distillation, the pH values of

Table 5. Physical properties of products produced over two catalysts

Sample	pH value	Density (g/mL)	Moisture content (%)	Viscosity (cP)	Heating value (MJ/kg)
Camelina oils	5.44±0.38	0.89±0.02	0.08±0.01	59.4±0.11	39.4±0
UCO	4.60±0.06	0.84±0.02	0.52±0.03	1.56±0.04	41.3±0.13
HF	5.50±0.14	0.83±0	0.06±0	1.00±0	42.8±0.13
DR	4.86±0.13	0.89±0.02	0.16±0.01	16.7±0.07	42.0±0.02
UCOZ	4.81±0.24	0.85±0.02	0.14±0.01	2.93±0.05	41.8±0.06
HFZ	5.30±0.24	0.78±0.03	0.07±0.01	1.03±0.01	42.8±0.03
DRZ	5.20±0.37	0.87±0.01	0.07±0	91.5±0.35	41.4±0.08

*UCO: upgraded camelina oils produced over ZSM-5; HF: hydrocarbon fuels produced over ZSM-5; DR: distillation residues produced over ZSM-5; UCOZ: upgraded camelina oils produced over ZSM-5-Zn; HFZ: hydrocarbon fuels produced over ZSM-5-Zn; and DRZ: distillation residues produced over ZSM-5-Zn

hydrocarbon fuels increased compared to upgraded camelina oils. The pH value of hydrocarbon fuels produced over ZSM-5-Zn was lower than that of hydrocarbon fuels produced over ZSM-5. For the distillation residues, they had a lower pH value than hydrocarbon fuels.

For the density, there was no big difference between upgraded camelina oils produced over ZSM-5 and upgraded camelina oils produced over ZSM-5-Zn. Compared to camelina oils, the upgraded camelina oils' density decreased. The density of an oil is related to its chemical structure and composition. After the catalytic cracking, the large molecules and complicated structures were converted into smaller molecules and simpler structures, respectively. Therefore, the upgraded camelina oils had a lower density than camelina oils. After the distillation, the densities of hydrocarbon fuels decreased further, especially for hydrocarbon fuels produced over ZSM-5-Zn. The density of hydrocarbon fuels produced over ZSM-5-Zn was lower than that of hydrocarbon fuels produced over ZSM-5. The densities of distillation residues were higher than upgraded camelina oils since the large molecules with high boiling points were remained in the distillation residues.

The water content of products is represented in Table 5. Water was one by-product during the catalytic cracking process. The free or bonded water in oils will cause the formation of free fatty acids, which could corrode the engine and fuel storage tank [38,39]. Upgraded camelina oils produced over ZSM-5-Zn contained a lower water content than that of upgraded camelina oils produced over ZSM-5. Compared to camelina oils, the upgraded camelina oils contained a much higher water content. This was because water was generated during the catalytic cracking process. After the distillation, the water content of hydrocarbon fuels was lower than 0.1%. The water content of hydrocarbon fuels produced over ZSM-5-Zn was slightly higher than that of hydrocarbon fuels produced over ZSM-5. Distillation residues produced over ZSM-5-Zn had a much lower water content than distillation residues produced over ZSM-5.

It is obvious from Table 5 that there was a big difference between the viscosities of upgraded camelina oils produced over ZSM-5 and upgraded camelina oils produced over ZSM-5-Zn. Viscosity is an important determining factor of the fuel quality and use that may significantly influence the performance of the pump and the fuel injector in engines. It is affected largely by the chemical structures of oils, such as chain length, chain branching, degree of unsaturation, molecular configuration (cis-trans, conjugation) and presence of oxidation products [40]. There was a higher area content of large molecules in upgraded camelina oils produced over ZSM-5-Zn, such as C_{19} and C_{21}, which might cause the higher viscosity compared to upgraded camelina oils produced over ZSM-5. Compared to camelina oils, the viscosity of upgraded camelina oils decreased apparently. In camelina oils, fatty acids with long chain length, complex chain branching, high degree of unsaturation and complicated configuration resulted in the high viscosity. After the distillation, the viscosities of hydrocarbon fuels decreased compared to upgraded camelina oils. However, there was no big difference between the viscosities of hydrocarbon fuels produced over ZSM-5 and hydrocarbon fuels produced over ZSM-5-Zn. The viscosities of distillation residues were much higher than upgraded camelina oils.

For the heating values, there was no big difference between upgraded camelina oils produced over ZSM-5 and upgraded camelina oils produced over ZSM-5-Zn. Compared to camelina oils, the heating value of upgraded camelina oils increased by about 5%. After the distillation, the heating value of hydrocarbon fuels further increased by about 3%. Compared to upgraded camelina oils, the lower oxygen content in hydrocarbon fuels might lead to their higher heating value. The heating value of hydrocarbon fuels produced over ZSM-5 was the same as that of hydrocarbon fuels produced over ZSM-5-Zn. For distillation residues, their heating values were lower than those of hydrocarbon fuels, which might be due to the higher oxygen content in distillation residues.

5. The Yield Rate of Products

Table 6 shows the yield rate of products produced over ZSM-5 and ZSM-5-Zn, respectively. The yield rate of upgraded camelina oils produced over ZSM-5-Zn was slightly higher than that of upgraded camelina oils produced over ZSM-5. After the distillation, the yield rate of hydrocarbon fuels produced over ZSM-5-Zn was

Table 6. The yield rate of products produced over two catalysts

Product	ZSM-5	ZSM-5-Zn
Upgraded oils (wt%)	62.5	63.9
Hydrocarbon fuels (wt%)	50.7	51.1
Distillation residues (wt%)	46.4	47.0

slightly higher than that of hydrocarbon fuels produced over ZSM-5. This might be attributed to the higher total acid sites in the ZSM-5-Zn catalyst than the ZSM-5 catalyst. Also, the yield rate of distillation residues produced over ZSM-5-Zn was slightly higher than that of distillation residues produced over ZSM-5. From these results, the incorporation of 3 wt% Zn^{2+} was helpful to increase the yield rate of hydrocarbon fuels. Maybe the effective chemical activation of Zn^{2+} assisted to obtain the higher yield rate of hydrocarbon fuels during the catalytic cracking of camelina oils.

6. GC Analysis

A typical GC analysis of the non-condensable gases generated from the catalytic cracking of camelina oils over two different catalysts is shown in Fig. 8. During the TCD signal analysis, there were several high noise peaks between the H_2 peak and CO_2 peak. In this study, these noise peaks were not shown in the TCD signal patterns. GC is a common method that is used to analyze gases produced during a variety of chemical processes. Several reactions occurred inside the ZSM-5 and ZSM-5-Zn catalyst, such as dehydration, decarbonylation and decarboxylation. These reactions removed oxygen atoms as H_2O, CO and CO_2 [18]. Apparently, the non-condensable gases were the co-products of the camelina oil upgrading.

During the catalytic cracking of camelina oils over two different catalysts, the non-condensable gases contained CH_4, C_2H_6, C_2H_4, C_3H_8, C_3H_6, C_4H_{10}, C_4H_8, C_5H_{12}, H_2, CO and CO_2. The production of CH_4 indicated that ZSM-5 and ZSM-5-Zn were capable of converting the triglyceride into the smallest hydrocarbon. Other small hydrocarbons (C_2-C_5) were produced during the complicated chemical reactions. These chemical reactions could be illustrated in the equations of (4) and (5) [11,41].

$$\text{Camelina oils } (C_xH_yO_z) \rightarrow \text{long-chain } C_xH_y + \text{long-chain oxygenated } C_xH_y \quad (4)$$

$$\text{Long-chain oxygenated } C_xH_y \rightarrow \text{long-chain } C_xH_y + H_2 + CO + CO_2 + H_2O \quad (5)$$

During the catalytic cracking of camelina oils, some generated hydrogen might react with unstable hydrocarbons to produce more stable products. For example, H_2 might react with C_2H_4 and C_3H_6 to produce C_2H_6 and C_3H_8, respectively. For CO and CO_2, they might be produced due to the cracking reactions of C_2H_4 or C_3H_6.

The total hydrocarbon compositions, C_1 to C_5, occupied an area content of 18.9% during the catalytic cracking of camelina oils over ZSM-5. The area content of CO was 2.03%. For the catalytic cracking of camelina oils over ZSM-5-Zn, the same hydrocarbon compositions were found in the non-condensable gases. The total hydrocarbon compositions occupied an area content of 3.92%, which was much lower than that in the non-condensable gases produced over ZSM-5. Furthermore, a lower content of CO_2 and CO was produced during the catalytic cracking of camelina oils over ZSM-5-Zn. However, more H_2 was produced during the catalytic cracking of camelina oils over ZSM-5-Zn. It indicated that there was less decarbonylation and decarboxylation, but more dehydration occurring during the catalytic cracking of camelina oils over ZSM-5-Zn.

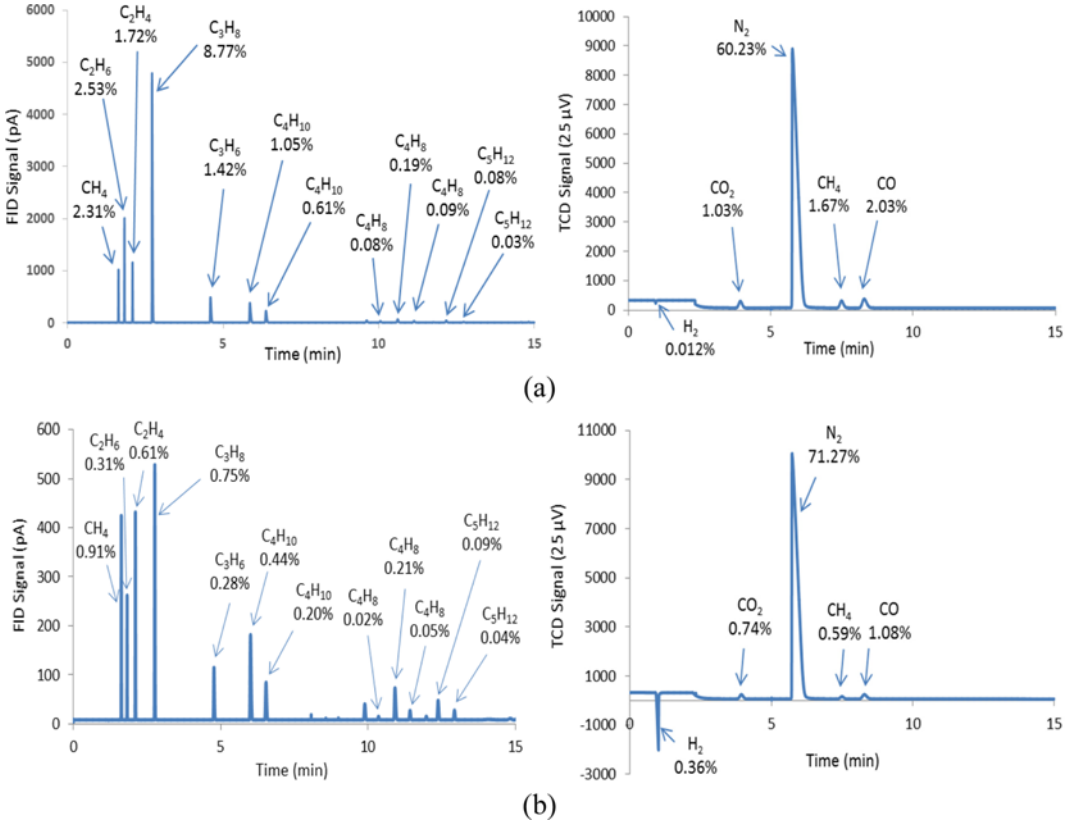

Fig. 8. A typical GC analysis for non-condensable gases produced from catalytic cracking of camelina oils over (a) ZSM-5; and (b) ZSM-5-Zn.

Alkanes and alkenes were the main hydrocarbon gases generated during the catalytic cracking of camelina oils over ZSM-5 and ZSM-5-Zn. The overall content of H_2 and CO in the non-condensable gases was relatively low. However, they might be worthy for future syngas collection and application.

CONCLUSION

ZSM-5 and its bifunctional zinc-loaded catalyst used for the cracking of camelina oils were compared by testing their performance in a fixed-bed reactor system. The loading of Zn^{2+} to ZSM-5 provided additional acid sites and increased the ratio of Lewis acid site to Brønsted acid site. High acid sites are vital for the catalytic cracking of inedible camelina oils to hydrocarbon fuels. The structure of the ZSM-5 catalyst remains intact after zinc-loading since zinc is only incorporated on the external surface of the ZSM-5 framework. All catalysts have similar surface morphologies and exhibit a combination of type I and type IV isotherm with both micropores and mesopores. However, zinc-loading is responsible for the physical changes of the ZSM-5 catalyst, such as surface area, pore volume and pore size. The used catalysts have the potential to be recycled for further use in the fixed-bed reactor system.

Upgraded camelina oils and distillation residues both mainly contain oleic acid, and hydrocarbon fuels mainly contain hydrocarbons. Distillation residues might be recycled for the further catalytic cracking since they contained a high content of fatty acids. Using ZSM-5-Zn as the catalyst, the pH value, heating value and yield rate of upgraded camelina oils increase slightly, compared to those using ZSM-5 as the catalyst. Also, the moisture and oxygen content in upgraded camelina oils produced over ZSM-5-Zn decrease. After the distillation, hydrocarbon fuels have lower density, viscosity, moisture content and oxygen content, but higher pH value and heating value than upgraded camelina oils. The incorporation of 3 wt% Zn^{2+} to ZSM-5 has improved the properties of hydrocarbon fuels to some extent compared to ZSM-5. For hydrocarbon fuels, their density and oxygen content are decreased while the yield rate is increased.

For the non-condensable gases, a lower content of CH_4, C_2H_6, C_2H_4, C_3H_8, C_3H_6, C_4H_{10}, C_5H_{12}, CO_2 and CO was produced during the catalytic cracking of camelina oils over ZSM-5-Zn compared to those over ZSM-5. However, more H_2 was produced during the catalytic cracking of camelina oils over ZSM-5-Zn. In the future, adding a higher amount of Zn^{2+} to ZSM-5 will be studied to evaluate the effect of zinc doping on the hydrocarbon fuel yield rate and quality through the catalytic cracking pathway. In addition, the operation conditions such as reaction temperature and liquid hourly space velocity will be optimized.

ACKNOWLEDGEMENTS

This study was funded by the U.S. Department of Transportation through NC Sun Grant Initiative under Grant No. SA0700149. The authors would like to thank Dr. Douglas Raynie, Ms. Changling Qiu and Ms. Shanmugapriya Dharmarajan for helping in the GC/MS analysis, Dr. Qiquan Qiao and Mr. Ashish Dubey for helping in the XRD, FTIR and SEM analysis, and Ms. Xiaomin Wang for helping in the BET analysis. The XRD equipment is supported by the NSF MRI grant (Award No. 1229577). All the support in experiment from Mr. Yang Gao, Yinbin Huang and Zhongwei Liu is gratefully acknowledged. However, only the authors are responsible for the opinions expressed in this paper and for any possible error.

SUPPORTING INFORMATION

Additional information as noted in the text. This information is available via the Internet at http://www.springer.com/chemistry/journal/11814.

REFERENCES

1. K. D. Maher and D. C. Bressler, *Bioresour. Technol.*, **98**, 2351 (2007).
2. A. Demirbas and H. Kara, *Energy Sources, Part A: Recovery, Utilization, and Environmental Effects*, **28**, 619 (2006).
3. T. M. Rao, M. M. Clavero and M. Makkee, *ChemSusChem.*, **3**, 807 (2010).
4. M. Chiappero, P. Do, S. Crossley, L. Lobban and D. Resasco, *Fuel*, **90**, 1155 (2011).
5. N. Zeeshan, X. Tang and W. Fei, *Korean J. Chem. Eng.*, **26**, 1528 (2009).
6. H. Wang, S. Yan, S. O. Salley and K. Y. Simon Ng, *Ind. Eng. Chem. Res.*, **51**, 10066 (2012).
7. J. Xu, J. Jiang, Y. Sun and J. Chen, *Bioresour. Technol.*, **101**, 9803 (2010).
8. H. Zhang, Y. Cheng, T. P. Vispute, R. Xiao and G. W. Huber, *Energy Environ. Sci.*, **4**, 2297 (2011).
9. J. Penzien, A. Abraham, J. A. Bokhoven, A. Jentys, T. E. Muller, C. Sievers and J. A. Lercher, *J. Phys. Chem.*, **108**, 4116 (2004).
10. A. Demirbas, *Energy Sources*, **25**, 457 (2003).
11. Z. Y. Zakaria, J. Linnekoski and N. A. Amin, *Chem. Eng.*, **207-208**, 803 (2012).
12. R. K. Sharma, M. Anand, B. S. Rana, R. Kumar, S. A. Farooqui, M. G. Sibi and A. K. Sinha, *Catal. Today*, **198**, 314 (2012).
13. H. Li, B. Shen, J. C. Kabalu and M. Nchare, *Renew. Energy*, **34**, 1033 (2009).
14. A. A. Boateng, C. A. Mullen and N. M. Goldberg, *Energy Fuels*, **24**, 6624 (2010).
15. A. E. Atabani, A. S. Silitonga, H. C. Ong, T. M. I. Mahlia, H. H. Masjuki, I. A. Badruddin and H. Fayaz, *Renew. Sust. Energy Rev.*, **18**, 211 (2013).
16. X. Zhao, L. Wei, J. Julson and Y. Huang, *Journal of Sustainable Bioenergy Systems*, **4**, 199 (2014).
17. T. R. Carlson, J. Jae, Y. Lin, G. A. Tompsett and G. W. Huber, *J. Catal.*, **2**, 110 (2010).
18. X. Zhao, L. Wei, J. Julson, Q. Qiao, A. Dubey and G. Anderson, *N. Biotechnol.*, **32**, 300 (2015).
19. X. Ren, N. Li, J. Cao, Z. Wang, S. Liu and S. Xiang, *Appl. Catal. A: Gen.*, **298**, 144 (2006).
20. R. Weingarten, G. A. Tompsett, W. C. Conner Jr. and G. W. Huber, *J. Catal.*, **279**, 174 (2011).
21. A. Zheng, Z. Zhao, S. Chang, Z. Huang, H. Wu, X. Wang, F. He and H. Li, *J. Mol. Catal. A: Chem.*, **383**, 23 (2014).
22. H. Jin, X. Wang, Z. Gu, J. D. Hoefelmeyer, K. Muthukumarappan

and J. Julson, *RSC Adv.*, **4**, 14136 (2014).
23. X. Zhao, L. Wei and J. Julson, *AIMS Energy*, **2**, 193 (2014).
24. Y. Huang, L. Wei, J. Julson, Y. Gao and X. Zhao, *J. Anal. Appl. Pyrolysis*, **111**, 148 (2015).
25. S. Bezergianni, S. Voutetakis and A. Kalogianni, *Ind. Eng. Chem. Res.*, **48**, 8402 (2009).
26. D. L. Trimm, *Appl. Catal. A: Gen.*, **212**, 153 (2001).
27. S. Kouva, J. Kanervo, F. Schüßler, R. Olindo, J. A. Lercher and O. Krause, *Chem. Eng. Sci.*, **89**, 40 (2013).
28. A. M. Camiloti, S. L. Jahn, N. D. Velasco, L. F. Moura and D. Cardoso, *Appl. Catal. A: Gen.*, **182**, 107 (1999).
29. G. Bagnasco, *J. Catal.*, **159**, 249 (1996).
30. F. Lónyi and J. Valyon, *Thermochim. Acta*, **373**, 53 (2001).
31. N. Kumar, L. E. Lindfors and R. Byggningsbacka, *Appl. Catal. A: Gen.*, **139**, 189 (1996).
32. S. Al-Khattaf, *Appl. Catal. A: Gen.*, **231**, 293 (2002).
33. Y. C. Sharma, B. Singh and J. Korstad, *Energy Fuels*, **24**, 3223 (2010).
34. J. Jae, G. A. Tompsett, A. J. Foster, K. D. Hammond, S. M. Auerbath, R. F. Lobo and G. W. Huber, *J. Catal.*, **279**, 257 (2011).
35. Y. Jiang, J. Juan, X. Meng, W. Cao, M. A. Yarmo and J. Zhang, *Chem. Res. Chinese U.*, **23**, 349 (2007).
36. M. Khatamian and M. Irani, *J. Iranian Chem. Soc.*, **6**, 187 (2009).
37. V. S. Yaliwal, S. R. Daboji, N. R. Banapurmath and P. G. Tewari, *Int. J. Eng. Sci. Technol.*, **2**, 5938 (2010).
38. E. Santillan-Jimenez, T. Morgan, J. Lacny, S. Mohapantra and M. Crocker, *Fuel*, **103**, 1010 (2013).
39. A. C. Rustan and C. A. Drevon, *Encyclopedia of Life Sciences*, 1 (2005).
40. H. Noureddini, B. C. Teoh and L. D. Clements, *J. Am. Oil Chem. Soc.*, **69**, 1189 (1992).
41. H. Zhang, R. Xiao, H. Huang and G. Xiao, *Bioresour. Technol.*, **100**, 1428 (2009).

Supporting Information

Catalytic cracking of inedible camelina oils to hydrocarbon fuels over bifunctional Zn/ZSM-5 catalysts

Xianhui Zhao, Lin Wei†, James Julson, Zhengrong Gu, and Yuhe Cao

Department of Agricultural and Biosystems Engineering, South Dakota State University, Brookings, South Dakota 57007, USA

(*Received 20 August 2014 • accepted 29 January 2015*)

1. Main Chemical Compositions of Products

Fig. S1 represents the GC-MS chromatograms resulted from products produced over ZSM-5 and ZSM-5-Zn catalysts. For upgraded camelina oils produced over ZSM-5 and upgraded camelina oils produced over ZSM-5-Zn, the same main chemical composition of oleic acid was assigned at the peak eluting at 9.038 min and 9.009 min, respectively. In addition, some other peaks appeared at the similar retention time. The oxidation of upgraded camelina oils would be affected by their fatty acid compositions such as unsaturated fatty acids. After the distillation treatment, hexane, 2,3-dimethyl-

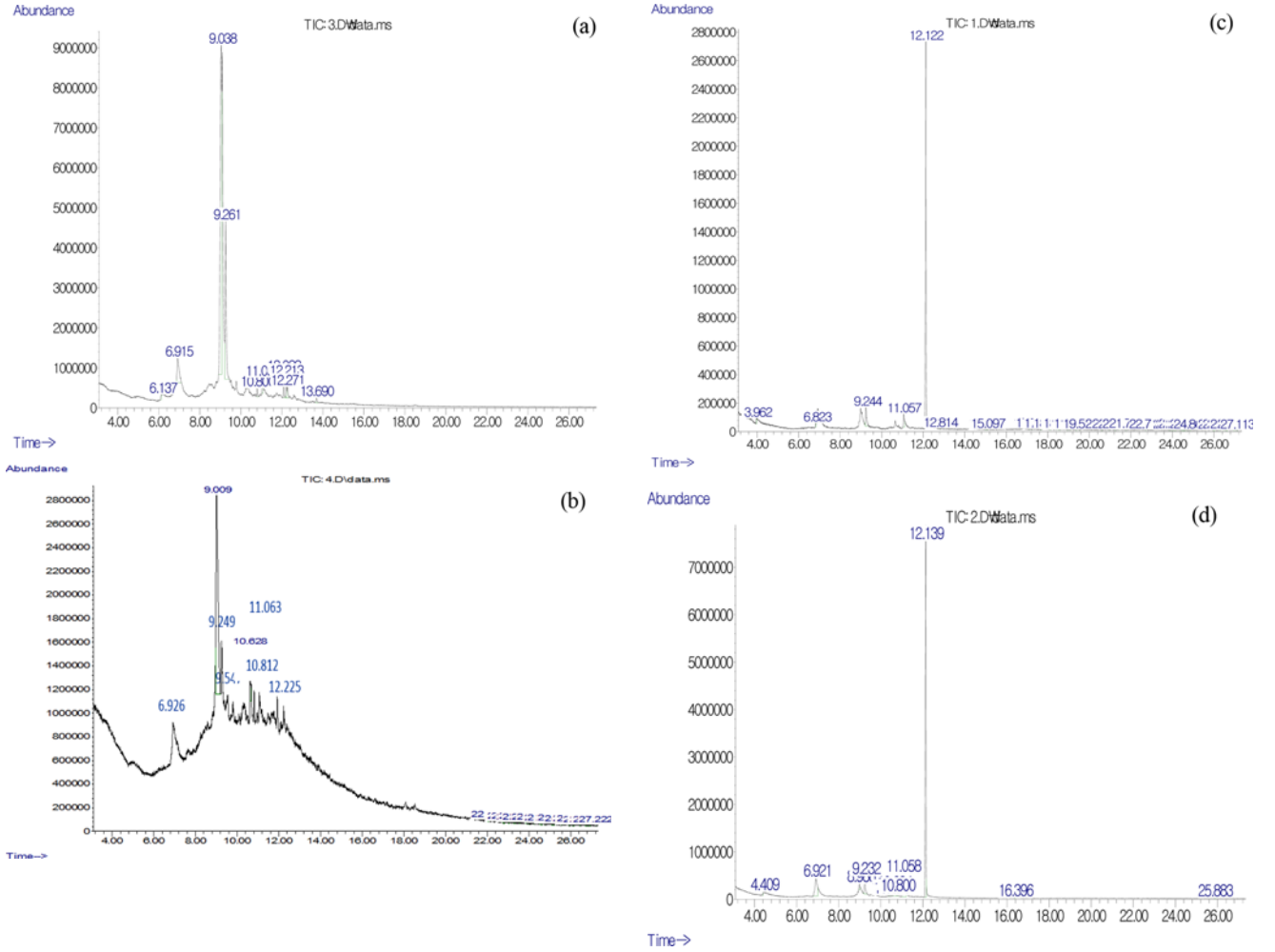

Fig. S1. GC-MS analysis of products: (a) UCO; (b) UCOZ; (c) HF; (d) HFZ; (e) DR; and (f) DRZ.

*UCO: upgraded camelina oils produced over ZSM-5; UCOZ: upgraded camelina oils produced over ZSM-5-Zn; HF: hydrocarbon fuels produced over ZSM-5; HFZ: hydrocarbon fuels produced over ZSM-5-Zn; DR: distillation residues produced over ZSM-5; and DRZ: distillation residues produced over ZSM-5-Zn.

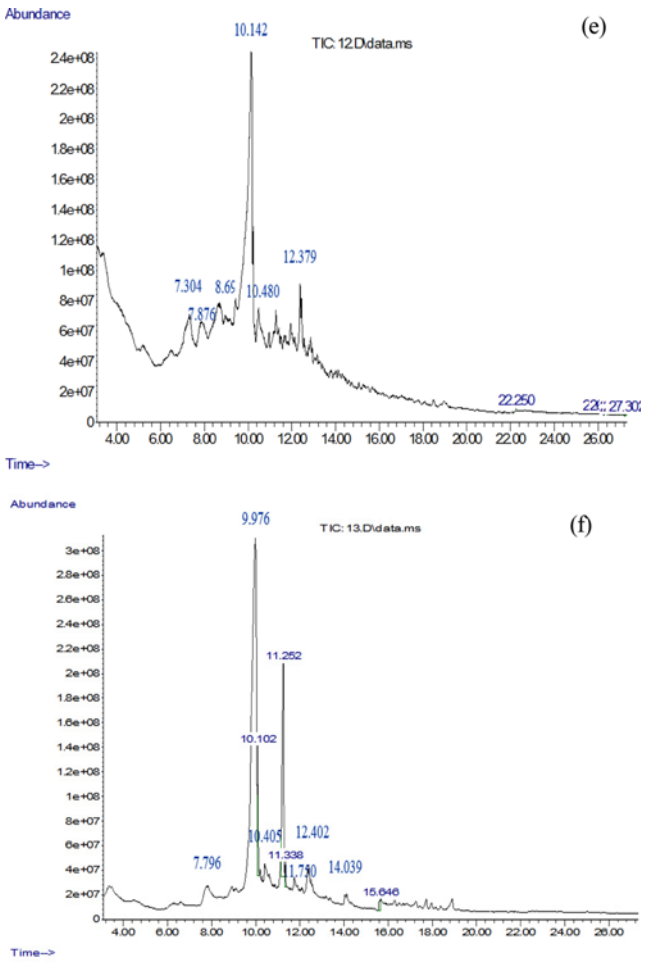

Fig. S1. Continued.

was the main chemical composition in both hydrocarbon fuels produced over ZSM-5 and hydrocarbon fuels produced over ZSM-5-Zn, eluting at 12.122 min and 12.139 min, respectively. For hydrocarbon fuels produced over ZSM-5, the peaks mainly appeared before 12.122 min. However, there were a number of small peaks assigned for the hydrocarbons after 12.122 min. For hydrocarbon fuels produced over ZSM-5-Zn, the peaks mainly appeared before 12.139 min and there were only two peaks appeared after 12.139 min. It indicated that the hydrocarbon fuels produced over ZSM-5-Zn contained fewer chemical compounds than hydrocarbon fuels produced over ZSM-5. In both distillation residues produced over ZSM-5 and distillation residues produced over ZSM-5-Zn, the main compound of oleic acid was found at the peaking eluting at 10.142 min and 9.976 min, respectively. The oleic acid could be recycled for the catalytic cracking in order to improve the hydrocarbon fuel yield rate.